Tellus (2002), 54A, 187–204
Printed in UK. All rights reserved

TELLUS
ISSN 0280–6495

Mechanisms of Antarctic katabatic currents near Terra Nova Bay

By S. DAVOLIO and A. BUZZI*, *ISAO-CNR, Via Gobetti 101, Bologna 40129, Italy*

(Manuscript received 19 February 2001; in final form 13 September 2001)

ABSTRACT

The evolution of Antarctic katabatic wind in the vicinity of Terra Nova Bay has been studied using a three-dimensional, hydrostatic, limited area model. Realistic simulations of a summer katabatic event, using different horizontal resolutions, have been performed by employing a sequential self-nesting procedure. The high-resolution orography data allow a description of the structure of the main valleys and of the two different flows descending from the broad Reeves Glacier and (with less accuracy) channelled into the much narrower Priestley Glacier valley, respectively. The mechanism of katabatic wind development has been investigated by means of a Lagrangian diagnostic study performed along trajectories flowing down from the above-mentioned glaciers. Heat balance and kinetic energy balance have been evaluated accurately in order to asses the characteristics of the two katabatic currents that may superpose once they reach the Nansen Ice Sheet.

1. Introduction

Starting from 1956, with the first simple model of Ball (Ball, 1956), the interest in the theoretical study of katabatic wind over Antarctica has progressively increased within the scientific community, particularly over the last 20 years. Recent advances have been achieved through several modelling studies which have simulated the spatial pattern of the wind field over the continent (Parish, 1988; Parish and Bromwich, 1990; Bromwich et al., 1990b), characterised by narrow coastal regions of strong convergence of the flow coming from the interior. Using high-resolution models, it has also been possible to investigate these confluence areas more accurately (Gallée and Schayes, 1994), relating the katabatic outflow to local phenomena such as the presence of polynyas (Gallée, 1997) or the mesocyclone development in the southwestern Ross Sea (Gallée, 1995; Gallée, 1996).

At the same time, observational studies have also progressed thanks to the increasing number of stations and instruments located over the continent, especially near the coast: Automatic Weather Stations (AWS), collecting surface weather data (Bromwich, 1989a; Bromwich et al., 1990a), radiosoundings and, during particular field phases, airborne instruments providing photography and measurements at different heights (Parish and Bromwich, 1989), as well as additional ground-based instruments, such as sodar or ultrasonic anemometer (Argentini et al., 1992; Argentini et al., 1995). Recently, the availability of high-resolution satellite imagery, useful for obtaining information on inaccessible areas, has allowed a general mapping of katabatic outflow through the warm signature in the thermal infrared (Bromwich, 1989b).

The great effort in modelling studies and data analysis is explained by the fact that katabatic winds exert an influence both on local and large-scale dynamics (Egger, 1985; Parish, 1992), as well as on most human activities and scientific experiments. The possibility of understanding the

* Corresponding author.
e-mail: a.buzzi@isao.bo.cnr.it

physical forcing mechanisms and predicting the intensity and duration of the katabatic outflow is of great scientific and practical importance.

Katabatic surface winds are generated over the Antarctic Plateau by strong radiative cooling, which is responsible for the development of a near-surface inversion layer. The cold, negatively buoyant air is driven downslope by the 'sloped-inversion force', whose name emphasises the topographic–thermodynamic forcing. It is possible to identify two different wind regimes: interior wind and katabatic wind. The former is a drainage flow over the Plateau resulting from a balance between the Coriolis and pressure gradient force, characterised by weak wind speed directed at large angles from the fall line. The latter is more intense and aligned with the fall line, and describes the topographically channelled flow over the steep coastal slopes, where the pressure gradient force is nearly balanced by friction. The convergence of the cold air into narrow glacial valleys, which takes place in regions of enhanced supply of negatively buoyant air, is the key feature of this strong and frequent wind field.

One of the main coastal areas of confluence is Terra Nova Bay, where the Reeves and Priestley Glaciers merge to form the Nansen Ice Sheet. The primary and wider route for the katabatic wind is from the Reeves Glacier across the Nansen Ice Sheet, but another current also blows down from the narrow valley of the Priestley Glacier. On an annual basis, the katabatic flow from the Priestley is warmer at the outlet, and consequently often passes above the flow from the Reeves, exhibiting complex behaviour and sometimes crossing the Northern Foothills (Bromwich et al., 1990a). Recent studies (Viola et al., 1999) have shown the existence of a short-timescale variation in the superposition between the two katabatic flows. In particular during summer, the situation can reverse within a daily cycle, as a result of different radiation budget regimes along the two flow paths that produce a diurnal modulation on the relative buoyancy. Therefore the wind from the Reeves Glacier can be warmer during daytime and flow over the Northern Foothills, this being facilitated by the underlying stream from the Priestley. The feature is confirmed by sodar measurements carried out at Terra Nova Bay. Statistical data analysis (Argentini et al., 1995) led to the conclusion that, during summer, the Priestley flow is usually confined to the first 400 m above the ground, and the katabatic current from the Reeves passes over the Northern Foothills and establishes the wind field recorded by the AWS at Terra Nova Bay.

In the present paper, high-resolution simulations of a summer katabatic event are examined in detail, also through comparison with observations, in order to better understand the physical mechanisms responsible for the phenomenon. An accurate diagnosis of trajectories within the katabatic flows is made in order to derive information on the basic properties of the two above-mentioned currents.

2. The model

The model used in this study is BOLAM (Buzzi et al., 1994; Buzzi and Foschini, 2000), version 2000. Model dynamics are based on hydrostatic primitive equations, with wind components u and v, potential temperature θ, specific humidity q, surface pressure p_s, as dependent variables.

The vertical coordinate is terrain-following (σ), with variables distributed on a non-uniformly spaced staggered Lorenz grid. The horizontal discretization uses geographical coordinates, with latitudinal rotation to minimise grid anisotropy, on an Arakawa C-grid. Second-order horizontal and vertical differencing is employed. The model implements an original second-order, forward–backward, advection scheme (Malguzzi and Tartaglione, 1999). The time scheme is split–explicit (forward–backward for gravity modes). A fourth-order horizontal diffusion of the prognostic variables (except for p_s), a second-order divergence diffusion and a damping of the external gravity mode are included. The lateral boundary conditions are imposed using a relaxation scheme (Davies, 1976; Leheman, 1993) that minimises wave energy reflection.

The surface and boundary layer scheme is based on the mixing length theory, with exchange coefficients computed as a function of the Richardson number. Different roughness lengths for momentum, heat and humidity are prescribed both over land and sea (depending on the surface wind speed in the absence of sea ice). A simplified sea ice parameterization is adopted in this application to Antarctica by assuming a constant-in-time sea ice distribution (fraction of sea covered by ice) and a prescribed surface temperature field and

roughness, simulating a thin ice layer. These simplified assumptions do not really affect the behaviour of the katabatic winds under study, although it has been shown (Gallée, 1997) that a proper description of the coastal polynyas may enhance the katabatic wind speed through an ice breeze effect. Surface processes (heat and moisture fluxes, snow cover evolution) are described using water and energy balances in a three-layer ground (including ice) model, where the deepest layer maintains prescribed temperature and water content. The albedo can change as a function of snow cover. Radiation balance is computed basically with Geleyn's scheme (Geleyn and Hollingsworth, 1979; Ritter and Geleyn, 1992), which deals with infrared and solar radiation interacting with clouds. Other physical parameterizations include dry adiabatic adjustment and moist convection (Kain and Fritsch, 1990).

The model has been tested and compared with many other mesoscale limited area models in the course of the COMPARE WMO project. Model intercomparison was conducted on a case of mid-latitude explosive cyclogenesis (Gyakum et al., 1996) and on a well documented case of flow over orography in the presence of lee waves and wakes (Georgelin et al., 2000). A specific adaptation of the model to the Antarctic environment, in particular concerning the treatment of sea ice and deep glaciers, has been made for the study of Antarctic coastal and barrier winds, by Buzzi et al. (1997). The model was applied to approximately the same area considered here, for simulating real meteorological events. A comparison with observations indicated satisfactory model behaviour.

The orography used in the simulations is derived from interpolation and smoothing of the 1 km (1/120°) resolution GLOBE Digital Elevation Model. The coastline data have been obtained from the same data set. The initial and lateral boundary conditions are supplied from ECMWF analyses at $0.5^\circ \times 0.5^\circ$ resolution. Hybrid model level data have been directly interpolated on the limited-area model grid. Sea ice cover, sea surface temperature and deep ice temperature are also obtained from the ECMWF analyses.

Sequential self-nesting has been employed to obtain high-resolution simulations. The initial and boundary variables are derived by interpolating the atmospheric, surface and ground (including ice) variables from the lower resolution runs to the higher resolution inner grids. Orography is defined at the resolution corresponding to the grid distance, after applying a spatial filter in order to reduce errors due to the sigma coordinates over steep terrain.

In the low-resolution experiments, a grid of 130×130 points was used, with a grid spacing of about 15 km and 36 vertical levels. In the nested experiments, the horizontal resolution is 3.3 km (140×140 grid points) with 48 vertical levels. Both domains are centred around 163°E, 74.5°S. The spacing between levels is variable, with the highest resolution in the lower portion of the atmosphere. In the low-resolution case, the lowest σ level is placed at about 15 m above the ground, with three levels located within 200 m. In the high-resolution case, the first σ level is at 8 m and there are four levels within 200 m above the surface.

The high horizontal resolution is required for the description of the orography, which plays a central role in the modulation of the katabatic winds. At the resolution of a few kilometres, the hydrostatic approximation is generally inaccurate. However, it should be considered that the topography of the area of interest presents valleys with longitudinal scales remarkably larger than the transverse scales and that the air flows mainly along such valleys rather than across them. An a posteriori scale analysis was performed on the flow. The condition which has to be satisfied for hydrostatic flow is $H/L^2 \ll 10^{-4}\,\mathrm{m}^{-1}$ (Bluestein, 1992), where H and L are the vertical and horizontal scales of motion. Bearing in mind the particular flow stratification due to the strong temperature inversion, typical length scales for the katabatic flow over the steep slopes are: $L \gtrsim 10$ km, $H \lesssim 1000$ m. The above condition is therefore easily met. Moreover, in the course of the Lagrangian diagnosis (presented in Section 4), consistency of the vertical acceleration term was checked. Therefore we assume that, although smaller-scale components of the motion (e.g. lee waves) may not be accurately described by the hydrostatic approximation, the general characteristics of the katabatic currents are still modelled in a realistic way.

3. Numerical simulations

Preliminary simulations were performed in order to ensure that the numerical model was

capable of generating katabatic outflow starting from rest conditions, with initially vanishing horizontal temperature gradient (Davolio and Buzzi, 2000). For the surface fields, the initial condition was obtained simply by interpolating the ECMWF analyses, verifying a particular early summer day, on the model grid. A vertical profile derived from the same ECMWF analyses was chosen and the whole atmosphere was made horizontally uniform by applying the selected profile everywhere. The wind was set to zero at all levels. With this particular initial condition, the build-up of the surface inversion turned out to be very slow, partially due to the summer season, but mainly due to a slow response of the surface layer to radiative cooling, as a consequence of the prescription of vanishing wind in the initial condition. In this case, in fact, the parameterized turbulent fluxes are very small near the surface. In order to speed up the cooling process and to generate a katabatic layer within the realistic timescale, the value of the Richardson number during the first few hours of integration was prescribed to be slightly less than the critical one. However, if started from a realistic condition, in the presence of a well developed inversion over the Plateau, the model requires a very short 'spin-up' time for the development of katabatic wind (Davolio and Buzzi, 2000), without any need of modifying the turbulence parameterization.

The present study takes into account the 72 h period from 31 December 1994, 00 UTC, to 3 January 1995, 00 UTC. These days have been chosen because during the summer 1994/95 a field experiment was carried out in the area of Terra Nova Bay: two stations were set up, one on the Reeves Nevè and another on the Nansen Ice Sheet, each equipped with a meteorological tower, a triaxial Doppler sodar and an instrumented mast, in order to provide high-resolution data on the vertical structure of the boundary layer (Viola et al., 1996). The analysis of the data recorded at the available AWS (Viola et al., 1999) showed the presence of pronounced katabatic wind within the selected period, from both the Reeves Glacier and Priestley Glacier.

As inferred from the ECMWF analyses, the synoptic situation at the beginning of the analysed period is characterised by a wide cyclonic belt over the Southern Ocean, in which a small-scale cyclone is embedded, located near Adelie Land. This depression is nearly stationary and weakens progressively in the time interval considered here. It is partly visible in the 700 hPa geopotential analysis field of Fig. 1(a). By 31 December, in the middle troposphere, a pronounced ridge, expanding from the Ross Sea, reaches the Antarctic Plateau. Consequently, an anticyclonic circulation develops over the continent [Fig. 1(a)]. By 1 January the weak large-scale gradient favours the development of the katabatic wind, associated with a strong pressure gradient at low levels directed across the coast. Over the Ross Sea, the wind coming from the continent experiences a rightward turn due to the southward large-scale flow along the coast. The high-pressure centre weakens and disappears during 2 January. In the meantime, another wide depression area begins to deepen over the north-eastern sector of the Ross Sea. It moves slowly southward and is associated with the onset of southerly wind over the Ross Ice Shelf.

The coarse-resolution (15 km) simulation, whose boundary conditions are updated every 6 h, is regarded mainly as an intermediate step required to drive the higher-resolution run. The interest of this study is concerned mainly with a local phenomenon, strongly driven by the topography. Consequently, high resolution is required, together with the best possible description of the orography. However, a number of peculiar features are displayed by the coarse simulation. First of all, it reproduces quite well the general synoptic circulation, the movements of the cyclones and the development of the southerly flow over the Ross Sea at the end of the period. Moreover, because

Fig. 1. (a) 700 hPa geopotential height interpolated from the ECMWF analyses, verifying 00 UTC, 01 Jan 1995. The contour interval is 20 m. Shading represents orographic height (interval 500 m). (b) Wind field at the lowest σ level for the low-resolution simulation, after 24 h of integration, verifying same time as in (a). Shading interval is 2.5 m s^{-1}. Maximum wind speed is about 12 m s^{-1}. The entire area corresponds to the model domain for the low resolution (15 km) integration. The two small squares represent the integration domain (outer) for the nested high-resolution (3.3 km) simulation and the output graphical area (inner) of the following figures, respectively.

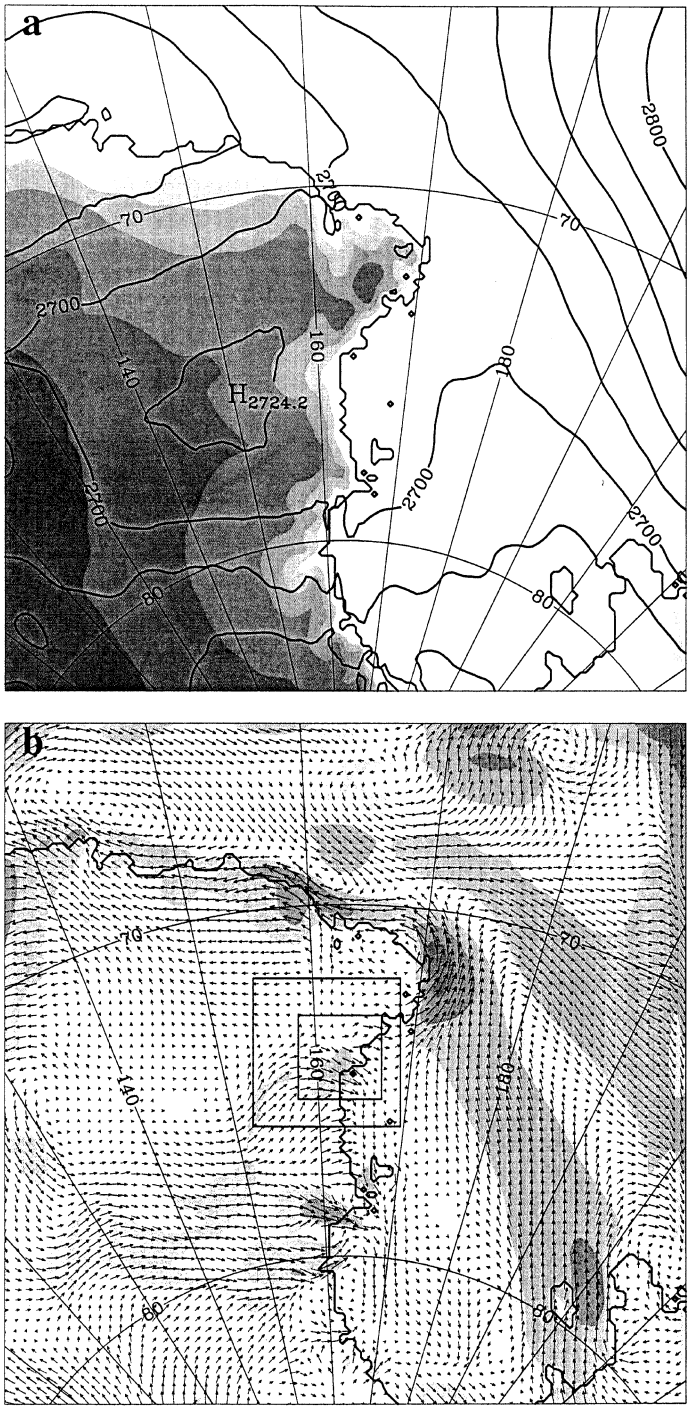
a
2800
2700
70
2700
160
140
H2724.2
180
2700
2700
80
b
70
160
140
180
80

of the higher resolution with respect to the ECMWF analyses, it also displays some interesting local features: after 24 h, the wind field at the first σ level [Fig. 1(b)] shows three narrow areas of strong convergence near the Ross Sea coast, which are well known as cold air drainage zones (Parish, 1988; Bromwich et al., 1990b). One of these regions, the northern one, corresponds to Terra Nova Bay; here the wind displays an increase in speed and a marked turn, becoming oriented in a direction which is typical of katabatic flow regimes in that area (270–300°).

For a detailed analysis and a quantitative comparison with observations, a high-resolution, 48 h simulation was performed, starting from 31 December 1994, 12 UTC. In this case the boundary conditions were updated every 2 h. Figure 2 shows the presence of four distinct topographically driven currents. The northern one flows over the Aviator Glacier valley, characterised by a north-westerly orientation in the vicinity of the coast. Another katabatic current, which is sustained by a wide confluence area on the Plateau, emerges from the David Glacier located near the southern boundary of the domain. In the middle of the displayed area, two distinct channelled streams flow over the valleys of the Reeves and Priestley Glaciers, reaching the Nansen Ice Sheet. The main flow comes from the Reeves valley because of the larger mass of air involved: indeed, the area of drainage upstream is considerably wider for the Reeves than for the Priestley Glacier. In the former case, in fact, the inflow extends up to more than 100 km over the Reeves Nevè area, which is larger than 10 000 km^2 [Figs. 1(b) and 2]. In the second case, the 'catch-

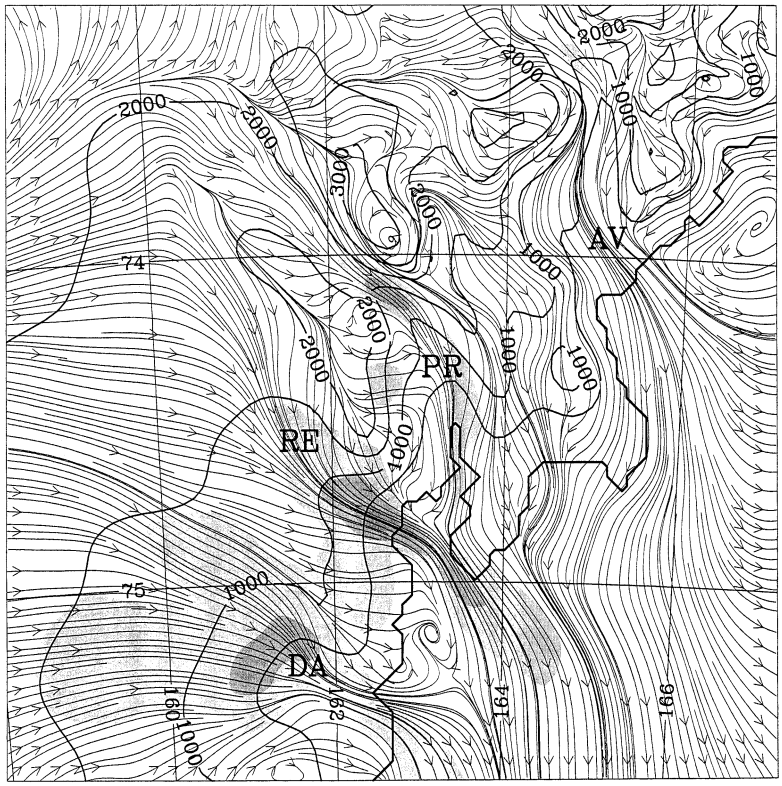

Fig. 2. Streamlines of wind at the lowest σ level after 12 h of the high-resolution simulation, verifying 00 UTC, 01 Jan 1995. The displayed area corresponds to the inner square of Fig. 1(b). AV, PR, RE and DA indicate, respectively, the Aviator, Priestley, Reeves and David Glacier valleys. Shading represents wind speed (interval 2.5 m s^{-1}). Elevation contours are plotted (thick lines, interval 500 m).

ment' area upstream of the Priestley valley is about one-fourth of the above value.

As already pointed out by Bromwich et al. (1990b), the deflection of the flow due to the mountains that separate the two valleys enhances the convergence over the Reeves Glacier [Figs. 2 and 3(a)]. The basic role played by the size of the upstream catchment basin in determining the temporal and spatial dimensions of the katabatic events is revealed clearly by the time evolution of the wind field near the surface [Figs. 3(a) and 3(b)]: over the Reeves Glacier the wind is more intense and affects a larger area for a longer time, compared to the flow along the Priestley valley. Note also that the general wind direction has changed over the Ross Sea, in response to changes in the large-scale circulation, but without affecting much the katabatic flow over the continent.

The orography employed in the high-resolution simulation provides an approximate description of the major valleys in the vicinity of Terra Nova Bay. In particular, it is possible to characterise to some extent also the flow in the narrow Priestley Glacier valley. Previous modelling studies (Bromwich et al., 1990b; Gallée and Schayes, 1994) did not represent the single valleys because of the lower resolution employed. Consequently, the smoothed topography did not resolve the coastal details, and the models produced only a broad katabatic flow from the Reeves Glacier (Bromwich et al., 1990b). However, even if it is now possible to identify the strong drainage over the Priestley Glacier valley, still higher resolution is probably required to describe more accurately the effects of the steep lateral walls in such a narrow 'canyon'.

Over the interior of the continent, the wind is directed with large angles from the fall line and the speed is quite low while, approaching the coast, enhanced wind speed is directed across the topography contour lines. This is consistent with a well known feature of the katabatic wind regime. Over the Reeves Glacier, the wind speed, at all model levels within the lower 200 metres, increases significantly at about 1200–1500 m surface elevation. In particular, the value of 15 m s^{-1} at the fourth σ level (about 170 m above the ground), obtained in correspondence to the 1200 m elevation contour (not shown), compares quite well with the aircraft measurements made by Parish and Bromwich (1989). The wind velocity further increases downstream, reaching its maximum just before reaching the coastline. The maximum speed is attained at about 90 m above the surface (corresponding to the third model σ level).

The features of the two katabatic jets can be better appreciated by looking at a meridional cross-section of total wind speed (Fig. 4), taken along a longitude passing through the interior of the Terra Nova Bay area [see Fig. 3(a) for the location]. It shows the signature of the flow over the Reeves valley (rightmost jet), at about 400 m surface elevation, before it reaches the glacier mouth, as well as the wind inside the Priestley Glacier valley (leftmost jet), at the 1500 m surface elevation contour, before it undergoes the marked southward turn towards the Nansen Ice Sheet. The cores of the katabatic jets are quite close to the surface in both cases. The asymmetrical pattern of the isotachs reveals the Coriolis force deflection that concentrates the katabatic flows on the left side of each valley, looking downwind (Bromwich et al., 1990b).

The dominant forcing mechanism of the katabatic flow, known as sloped-inversion force, depends on the cold near-surface layer, characterised by a strong vertical temperature inversion. As can be seen in Fig. 5, the model is able to reproduce the stratification of the katabatic layer: a very stable layer is present just over the surface, while above the static stability is much weaker and a wave is present over the steepest descent region. This kind of phenomenon has been observed in cases of strong katabatic events (Pettré and André, 1991).

The surface sensible heat flux is shown in Fig. 6. The downward heat transfer reaches its maximum in the portions of the Reeves and Priestley Glacier valleys closer to the coast, due to the combination of strong wind speed and relatively high air temperature near the surface, due to the adiabatic compression. Down from the Reeves Glacier, the heat flux maximum is about 150 W m^{-2}. The pattern of sensible heat flux is similar to that of the satellite observed signature in the thermal IR images, which reveals the presence of relatively warm surface (Bromwich, 1989b; Parish and Bromwich, 1989).

3.1. *Comparison with AWS data*

We consider here a direct intercomparison between available AWS observations and model

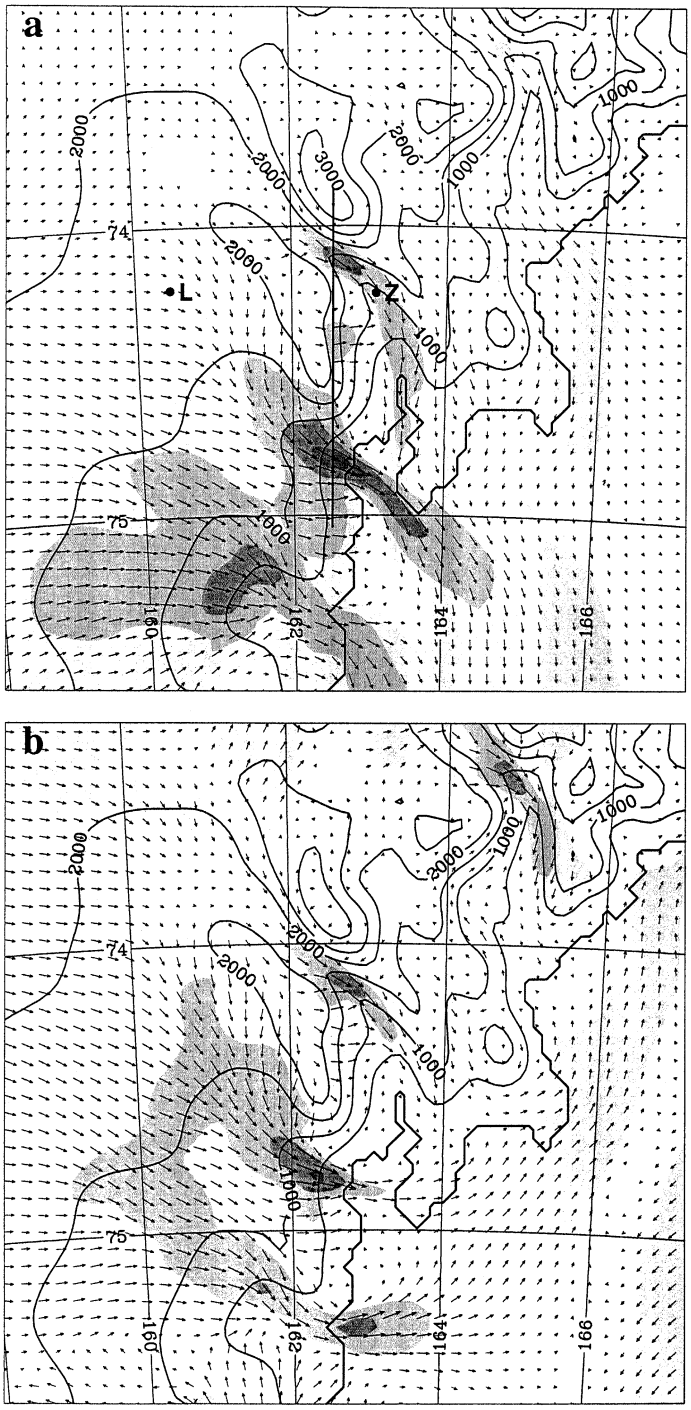
a
b
L
Z
74
75
160
162
164
166
1000
2000
3000

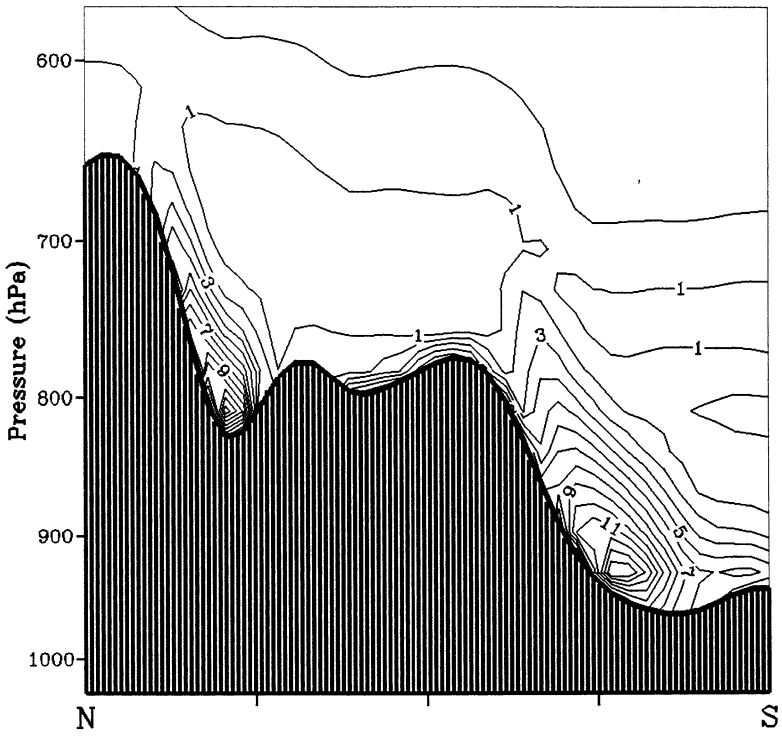

Fig. 4. Meridional cross-section of total wind speed, along the line shown in Fig. 3(a), verifying the same time as Fig. 3(a). The contour interval is 1 m s^{-1}. The interval between thick marks on the horizontal axis corresponds to 10 grid meshes (33 km).

output data. Agreement is limited, in principle, by the poor quality of the initial analyses over the Antarctic continent. Moreover, the AWS are quite sparse and, in some cases, are located in areas that may not be very representative for model intercomparison, due to the local topographic characteristics. Notwithstanding this, important information can be obtained by the comparison. Starting from the interior, over the Reeves Nevè, the station 'Lynn' [for location see Fig. 3(a)] displays, in the period of interest, a weak wind around 5 m s^{-1}, mostly directed between 270° and 300° [Fig. 7(a)]. This is a characteristic of the flow in that area, as revealed by several AWS data analyses (Bromwich et al., 1990a; Argentini et al., 1995): the wind is strongly affected by the local slope direction. In the simulation (same figure), the behaviour of the flow, nearly constant in intensity and direction, is well caught by the model. The slight difference in direction probably arises from an imperfect reproduction of the local orography.

The lack of an accurate topographic representation affects more severely the model results within the Priestley Glacier valley: the modulation of the wind is in some agreement with the data, but the model speed is remarkably lower [Fig. 7(b)] when compared with AWS 'Zoraida' [see location in Fig. 3(a)]. In contrast, the model wind direction is in good agreement with the observed direction

Fig. 3. As Fig. 2 but for the wind vectors at the lowest σ level. (a) After 12 h of integration, verifying 00 UTC, 01 Jan 1995. Maximum wind speed is about 11 m s^{-1}. The dots with symbol L (Lynn) and Z (Zoraida) indicate the AWS locations. The straight line shows the position of the cross-section plotted in Fig. 4(b) after 36 h of integration, verifying 00 UTC, 02 Jan 1995. Maximum wind speed is about 10 m s^{-1}.

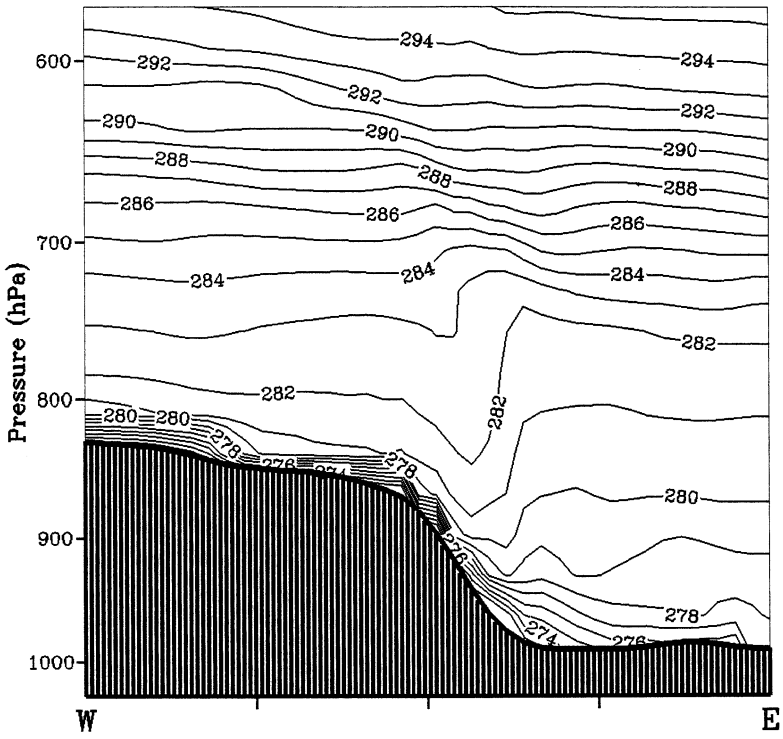

Fig. 5. Zonal cross-section of equivalent potential temperature at the longitude corresponding to the Reeves Glacier outlet, after 24 h of integration, verifying 12 UTC, 01 Jan 1995. The contour interval is 1 K. The interval between thick marks on the horizontal axis corresponds to 10 grid meshes (33 km).

during the katabatic wind period. After about 6 UTC on 2 January, both the wind speed and direction quickly change, marking the end of the katabatic episode. The cessation of the katabatic wind is represented by the model, although the decrease in wind speed is more gradual than in the observations. In summary, it appears that the model is partly able to capture the topographic channelling of the Priestley valley, even if the valley itself is too narrow to be properly described at the employed resolution.

At both 'Lynn' and 'Zoraida' the model reproduces the daily cycle which is more prominent over the Reeves Nevè than over the Priestley Glacier. However, while at 'Zoraida' the model temperature is in good agreement with the observed temperature (differences stay within 2 K), at 'Lynn' it is significantly colder during the warmest period of the day (up to 6 K), implying a reduction of the diurnal oscillation.

Over the Nansen Ice Sheet, the simulated wind speed is between 10 and 13 m s^{-1}, and does not seem to fluctuate in intensity and direction, as displayed by the AWS 'Sofia' data (not shown). Moreover the katabatic flow does not strengthen during the second day as it does in reality. In such a small domain, this may be due to the lack of a three-dimensional large-scale circulation that can supply cold air over the Plateau to sustain the katabatic winds for a long time.

An analysis of the potential temperature over the Reeves Nevè (at 'Lynn') and Priestley Glacier (at 'Zoraida') was employed by some authors (Bromwich et al., 1990a; Viola et al., 1999) to asses the buoyancy characteristics of the two flows downstream over the Nansen Ice Sheet, assuming nearly adiabatic conditions. With this assumption, such analysis would lead us to the conclusion that the simulated flow from the Reeves Glacier valley is colder during most of the day, although for a few hours the situation is reversed. In fact, by 1 January, between 06 and 12 UTC (afternoon

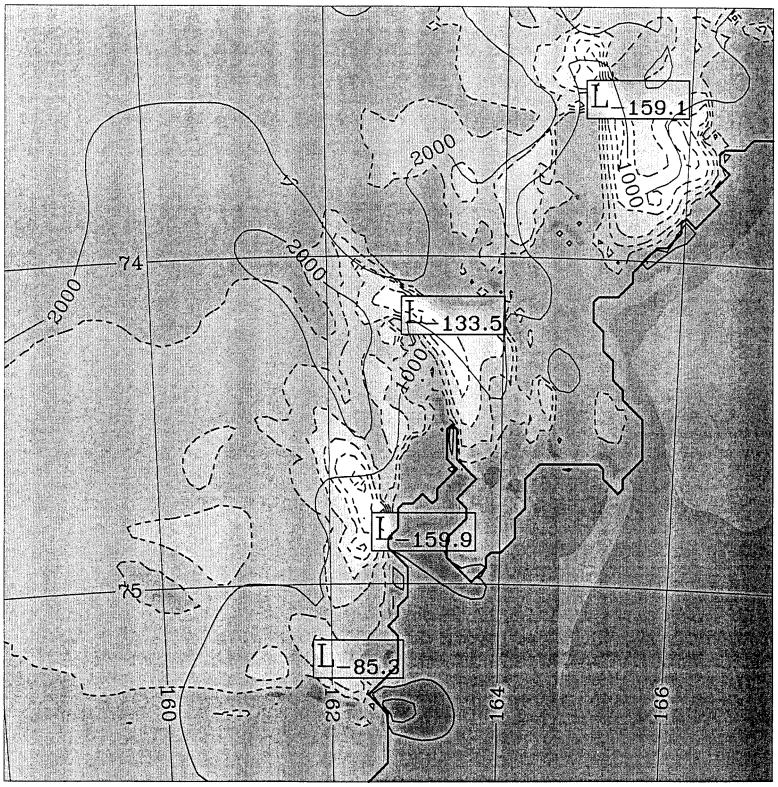

Fig. 6. Sensible heat fluxes (positive upward) after 24 h of integration, verifying 12 UTC, 01 Jan 1995. Shading interval is 25 W m^{-2}. Dashed lines correspond to negative values (downward flux). Elevation contours are plotted (thick lines, interval 1000 m).

LT), the potential temperature at the lowest σ model level, at 'Zoraida' AWS, is slightly lower than the potential temperature corresponding to 'Lynn' AWS. This result is in agreement with the recent study on the katabatic winds in Terra Nova Bay area of Viola et al. (1999), but it cannot be used to assess the relative buoyancy properties of the two katabatic flows, when they reach the Nansen Ice Sheet, for a number of different reasons. First, this kind of analysis is based on the assumption of an adiabatic descent, which is not confirmed in our model simulation, where the specific entropy changes substantially following the air motion over the steep coastal slopes, as will be shown in the diagnosis presented in Section 4.1. Second, the potential temperature changes differently during the descent in the two valleys. Third, the simulated flow that reaches the Nansen Ice Sheet from the Priestley Glacier is very weak. Probably due to the limitations in the orography representation, it hardly intercepts the main flow from the Reeves Glacier and therefore it is not possible to verify the superposition features from the model results. Fourth, additional experiments made in this context have shown that the thermal characteristics within the Priestley Glacier valley are quite dependent on the surface distribution of the incoming short wave radiation, taking into account the presence of the very steep valley sides and the low declination of the sun. When a realistic shadow is imposed inside the valley (not present in the formulation of the model used for the experiments described above), the daily cycle amplitude is reduced and the potential

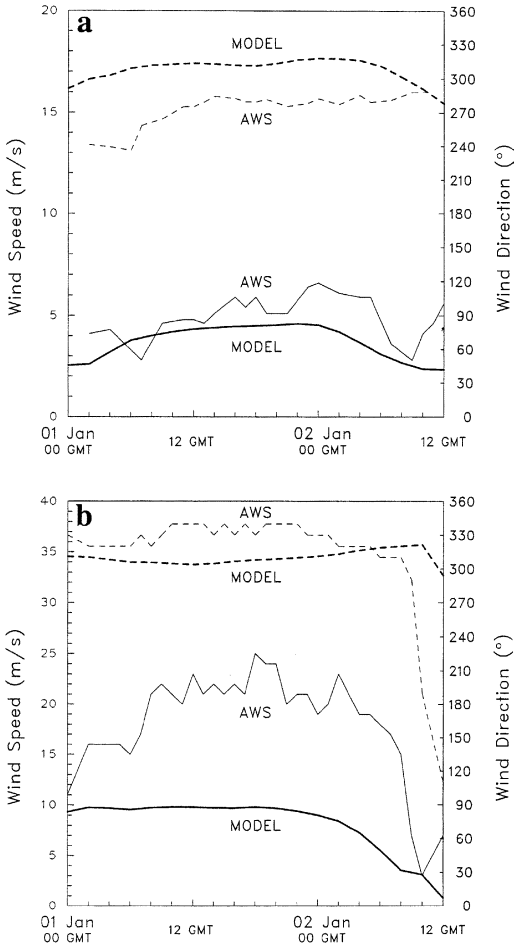

Fig. 7. Comparison of wind speed (solid lines) and wind direction (dashed lines) between AWS observations in Lynn (a) and Zoraida (b) and corresponding model closest grid points.

temperature at the first model level decreases by about 3 K. This affects, of course, the buoyancy characteristics of the flow.

4. Lagrangian diagnostics

With the aim of studying in more detail the physical characteristics of the two katabatic currents that reach the Nansen Ice Sheet, a diagnosis was performed, based on the evaluation of the contributions to the kinetic energy balance and to the heat balance along the trajectory of parcels flowing near the surface. Within the katabatic flow from both the Reeves and Priestley Glaciers, quasi-two-dimensional forward trajectories were calculated, over the first σ level, for parcels moving from the interior and reaching the coast. In order to justify the approximation of quasi-two-dimensional trajectories over the lowest sigma level, it was verified that the vertical velocity $\dot{\sigma}$ and the vertical advection remain very small. Moreover the streamlines displayed in Fig. 8 reveal that just over the steep slopes the flow is really almost parallel to the ground. Over the entire period characterised by the presence of katabatic outflow, only trajectories closely related in space were chosen, in order to obtain a coherent sample. Therefore, the mean analysis presented below was made on parcels that nearly follow the same route, taking approximately the same time to reach the coast.

4.1. Heat balance

For each trajectory, at time intervals of about 20 min, contributions to the potential temperature were calculated. Contributions due to horizontal diffusion, vertical diffusion, radiation and vertical advection were stored together with other physical quantities, such as sensible heat flux at the surface, wind speed and direction, potential temperature and temperature.

The heat balance equation for the potential temperature θ is:

$$\frac{\mathrm{d}\theta}{\mathrm{d}t} = \frac{\partial\theta}{\partial t} + \frac{u}{a\cos\phi}\frac{\partial\theta}{\partial\lambda} + \frac{v}{a}\frac{\partial\theta}{\partial\phi} + \dot{\sigma}\frac{\partial\theta}{\partial\sigma} = K_\theta + F_\theta \tag{1}$$

where K_θ stands for the dissipative horizontal processes and F_θ represents the remaining diabatic contributions. They include vertical turbulent diffusion, radiation and phase changes of water (the latter not relevant in our case). In eq. (1), u, v and $\dot{\sigma}$ are the velocity components in the σ coordinates, a is the earth radius, and ϕ and λ are rotated longitude and latitude.

Down from the Reeves Glacier, during the 24 h period between 1 and 2 January, 00 UTC, the katabatic flow was nearly steady and different trajectories were analysed. Since all the trajectories displayed similar spatial and temporal behaviour, an averaged analysis of the contributions to the potential temperature balance was performed.

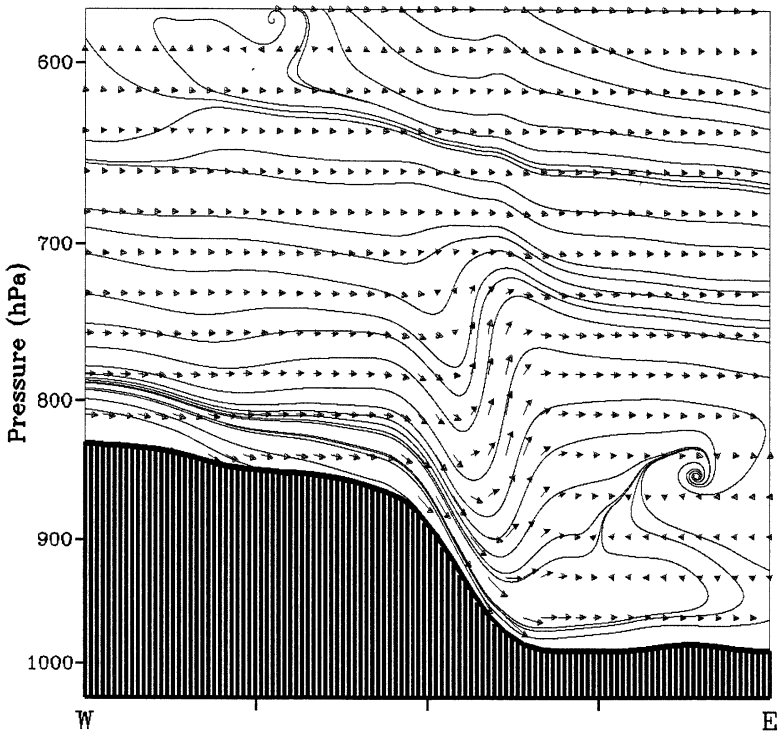

Fig. 8. As Fig. 5 but for wind vectors (u, w) and corresponding streamlines. The maximum wind vector corresponds to about 13 m s^{-1}.

Looking at the temperature evolution [Fig. 9(a)] along the descent, it is possible to distinguish three different regions. Over the gentle slope of the Plateau, where the wind speed is moderate [Fig. 9(b)], the turbulent exchanges between the surface ice and the atmosphere are negative (the surface cools the air above) but not large in magnitude [Fig. 9(c)]. Consequently, potential temperature decreases very slowly, in a quasi-adiabatic regime.

The radiative cooling of the iced ground is more efficiently transferred to the air above the slope along the steepest part of the descent, where the increasing wind speed strongly enhances the magnitude of the turbulent heat flux. Although the descending air becomes warmer because of the adiabatic compression, its potential temperature decreases as a result of the strong vertical mixing. This behaviour has already been observed in the course of instrumented aircraft flights over the Reeves Glacier valley (Parish and Bromwich, 1989) during a katabatic event: a dramatic increase in wind speed and temperature, corresponding to a decrease in potential temperature, was observed. This phenomenon is reproduced in our model simulations as shown in Figs. 9(a) and 9(b).

Once the parcel reaches the coastline, just after leaving the area of maximum wind speed, the heating contribution of vertical diffusion becomes positive, inducing an increase in potential temperature. This is mainly due to the underlying warmer sea.

All along the slope, the main contribution to the potential temperature variations at the lowest model level comes from vertical diffusion [Fig. 9(c)]: the air is cooled because of the strong negative vertical potential temperature gradient between the first σ level and the ground. On average, this contribution lies in the range $(2\text{–}7) \times 10^{-4}$ K s^{-1}, and is strongly modulated by the wind speed, since the mixing processes are enhanced as the wind speed increases near the surface. On the other hand, the daily radiation cycle does not play an important role in shaping

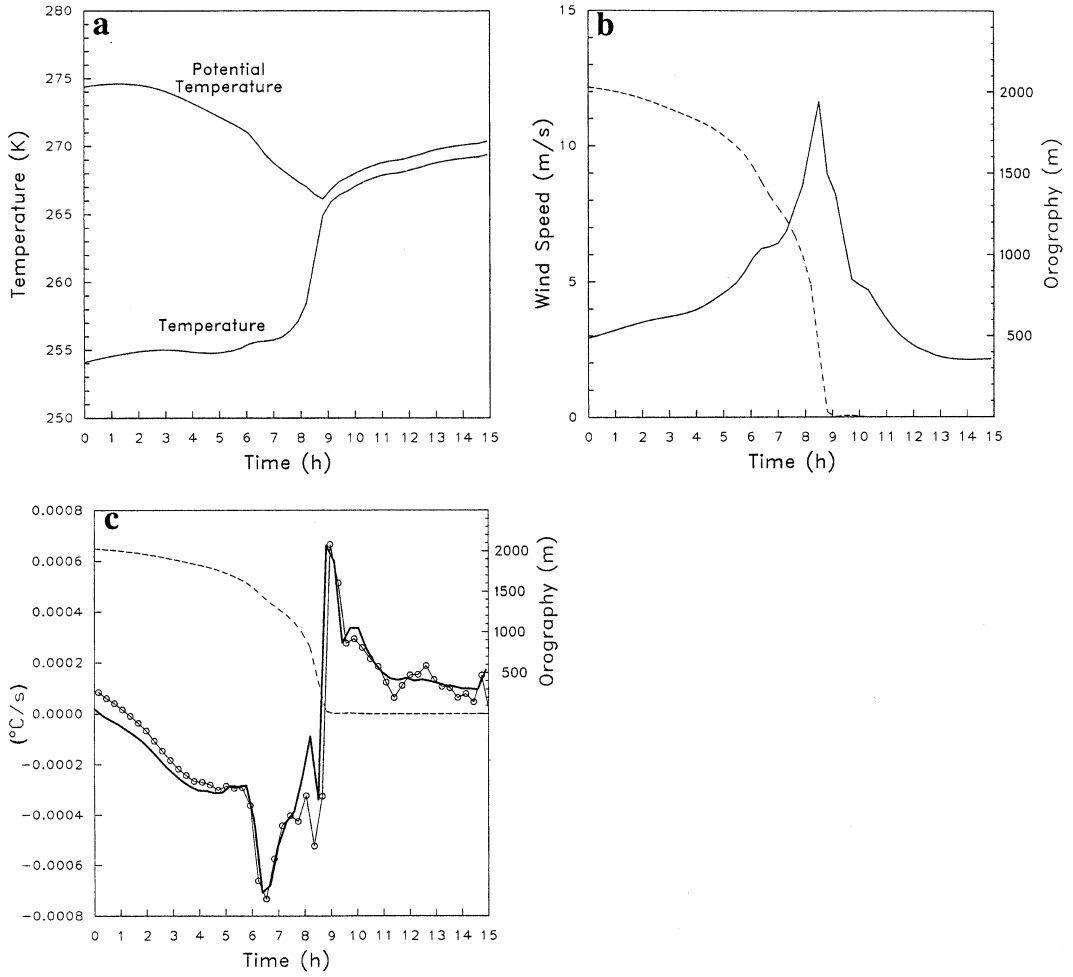

Fig. 9. Plots of quantities derived from diagnosis of trajectories for the Reeves Glacier (see also text). (a) Temperature and potential temperature. (b) Wind speed (solid line) and height (dashed line). (c) Heat balance; $d\theta/dt$ (line with circles) and contribution of the vertical diffusion (solid line). The dashed line represents the orography.

the potential temperature variation in the free atmosphere, and its contribution varies between $\pm 10^{-4}$ K s^{-1}.

As expected, the surface heat fluxes (see for example Fig. 6) reflect the behaviour of the vertical diffusion, being strongly negative (downward) inland and positive (upward) offshore. The largest magnitude in absolute mean value of about 100 W m^{-2} is reached in correspondence to the maximum wind velocity.

The validity of the same two-dimensional diagnosis for the Priestley Glacier is limited by the fact that the valley is very narrow, and therefore is not properly described by the model. Moreover, the katabatic flow is not steady enough to give coherent trajectories as for the Reeves Glacier: since the katabatic wind does not persist for much time all along the Priestley valley, there are only a few computed trajectories that follow nearly the same path from the interior to the Nansen Ice Sheet. Within a period of 12 h, the analysed trajectories show that the main contribution to the heat balance comes from the vertical diffusion, as in the Reeves case. Inside the valley it is generally negative, modulated in intensity by the wind speed, while at the outlet of the glacier

it becomes slightly positive. During their descent, air parcels display an increase in temperature and a decrease in potential temperature, as already observed in the Reeves Glacier. The flow from the Priestley Glacier reaches the Nansen Ice Sheet with a very low speed, and the model trajectories do not intersect those from the Reeves. Thus, it is not possible to analyse in detail the superposition of the two katabatic flows in our simulations.

4.2. Kinetic energy balance

By multiplying the horizontal momentum equation by $\vec{V}$ a balance equation for kinetic energy is obtained:

$$\underbrace{\frac{1}{2}\frac{\mathrm{d}|\vec{V}|^2}{\mathrm{d}t}}_{A} = \underbrace{-\vec{V}\cdot\nabla\Phi}_{B} + \underbrace{\vec{R}}_{C} \qquad (2)$$

where $\vec{V} = (u, v)$ is the horizontal velocity, Φ is the pressure force term and $\vec{R}$ includes the dissipative processes. The left-hand side is calculated along the two-dimensional trajectory using parcel velocity. The term containing the pressure gradient is available from the model, averaged over a time step of about 20 min. The dissipation term is computed as a residual.

The kinetic energy balance terms were analysed for both the Reeves and Priestley trajectories. In the former case, as mentioned above, it is possible to perform an averaged analysis using an ensemble of coherent trajectories. Figure 10(a) shows that the pressure gradient force increases its magnitude when approaching the coast, where the slope becomes steeper. At the same location, the wind velocity grows very rapidly [Fig. 9(b)] and consequently the kinetic energy increment reaches its maximum. Being associated with the maximum wind speed, kinetic energy dissipation becomes large and the temperature of the parcel increases, as shown in Fig. 9(a), together with the kinetic energy decrease. This result, in agreement with Parish and Waight (1987), indicates that the wind regime over the steep coastal slopes is characterised essentially by a balance between the pressure gradient force and frictional dissipation.

The balance for the Priestley seems more complex, with two separate peaks in the pressure gradient force present in Fig. 10(b). To explain this behaviour, the particular shape of the topographical channel has to be borne in mind. Indeed, in the analysed trajectories, the wind reaches the maximum speed along the slopes just before the sharp turn of the valley. In Fig. 10(b) this coincides with the first peak: the kinetic energy displays a positive increment mainly due to the pressure gradient force. Subsequently, the sudden change in the direction of the valley is associated with a kinetic energy decrease, because friction exceeds the pressure gradient force. After the turning, the wind tends to increase weakly again over the coastal slope, but once it has reached the Nansen Ice Sheet, the pressure gradient force ceases.

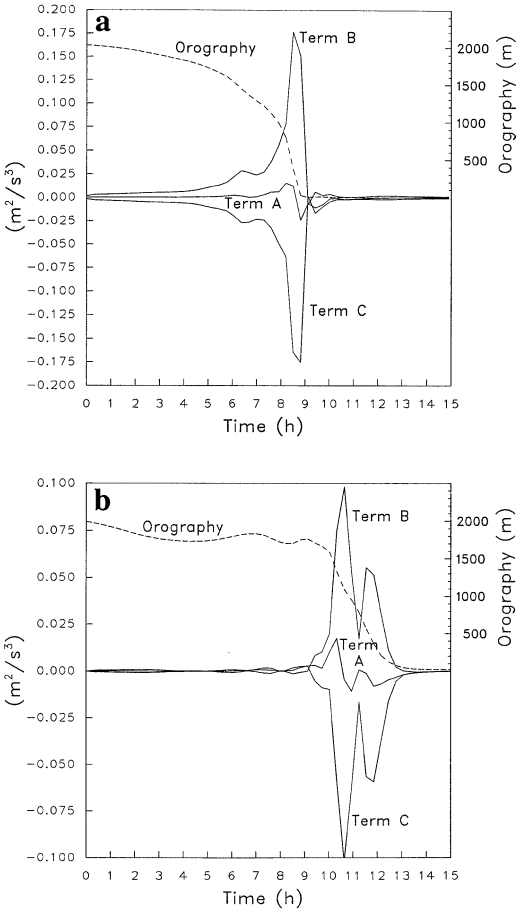

Fig. 10. As Fig. 9 but for the kinetic energy balance for the Reeves Glacier (a) and Priestley Glacier (b). Terms *A*, *B* and *C* are as labelled in eq. (2) (Section 4.2).

5. Conclusions

Katabatic winds in Antarctica are a dominant climatic feature of the coastal and near coastal areas. However, they are strongly modulated in intensity both in time, due to the seasonal cycle and the synoptic scale meteorological variability, and in space, due to the presence of deep glacial valleys, draining dense air from the Plateau and driving it towards the coast. It is at the outlet of these valleys to the sea that the highest wind speeds are generally observed. The area of Terra Nova Bay offers an interesting example of complex coastal topography, in which several valleys of different length, width and orientation are associated with distinct katabatic streams and flow regimes. Given the same large scale forcing, the response of each individual valley in terms of strength and thermal characteristics of the katabatic current may vary in time. An accurate prediction of katabatic wind onset and decay is therefore made more difficult by the complex local topography, which regulates the flow through a number of different effects.

The katabatic wind regimes in Terra Nova Bay have been the subject of numerous observational studies. In the present numerical study, aimed at understanding the effects of topographic features, we have focused our attention on two quite different glacial valleys, namely the Reeves and Priestley Glaciers. A mesoscale meteorological model has been applied both to idealised conditions (generation of katabatic wind starting from rest, in the absence of large-scale forcing) and realistic conditions, in a particular situation in which observations were available. Two different grid resolutions have been employed. At about 15 km grid distance, only the widest katabatic currents are simulated, while the narrower valleys like the Priestley are described by the model at resolutions of 3–4 km at most.

The differences in the properties of cold air drainage in the catchment areas over the Plateau and the channelling effects downstream have been described and compared. Over the Reeves Glacier, the large drainage area upstream contributes to forming an intense descending current that continues for several tens of kilometres offshore, as already observed by Bromwich (1989a, b). Simulated values of both low-level temperature and wind compare well with the available observations for the period considered. In contrast, the Priestley Glacier possesses a much smaller upstream catchment area, in which the thermal characteristics of the air mass may differ from those of the Reeves Nevè, due to different wind speed and thermal balance. These elements, however, are not related to detailed topographic features and therefore should be described also in comparatively low-resolution simulations. This is no longer true for the dynamical and thermal budgets within the long and very narrow Priestley valley. The steep lateral walls of such valley force 'channelling' of the flow that modifies its dynamical characteristics, like horizontal and vertical shear and consequent turbulent properties, including lateral frictional effects. These factors, due to the strong nonlinearity associated with the katabatic flow regime, may strongly alter the momentum and heat budgets with respect to the wide valley configuration case. We have shown above that the strong speeds observed within the Priestley valley by AWS are not easily simulated, probably due to the smoothed representation of the valley topography. A more realistic simulation would require, in this case, a much better spatial resolution. Another difference between the two valleys considered here is related to their slope, which in the Reeves is about twice that in the Priestly. This effect should act in favouring larger wind speed in the former than in the latter. For both the Reeves and Priestley, the maximum wind speed is attained, both in our experiments and in the observations, in correspondence to the largest steepness of the valley floor.

In addition to the above dynamical effects, during summer the steep valley walls may also shadow part of the valley bottom from solar radiation, thus increasing the near surface cooling and enhancing the wind speed in response to enhanced negative buoyancy (Viola et al., 1999). In this regard, a strong sensitivity of the maximum wind speed to low-level temperature was found in the model experiments, although in all cases the Priestley flow weakens more rapidly at the outlet than the Reeves flow.

The model results have been used to diagnose, in a Lagrangian perspective, the heat and kinetic energy balances of the katabatic flow in the two different valleys. In both cases, the entire path of the katabatic flow is characterised by diabatic cooling of air in response to radiative net heat

loss of the surface and rapid vertical mixing, the latter being strongly enhanced by the wind intensity. Although potential temperature of an air parcel decreases, its absolute temperature increases along the trajectory due to the rapid descent. The contribution of vertical diffusion is such that the flow is far from being adiabatic. Sharp transitions occur when the currents reach the coastline: low-level diabatic cooling is replaced by warming and the wind speed drops quickly.

The analysis of the kinetic energy balance indicated that the work done by the downslope pressure gradient force in the region of maximum terrain slope is very strong but is largely balanced by turbulent dissipation. Although it was among the original aims of the study, it was not possible, at least with the present model set up, to asses the diurnal alternation of the two currents at the outlet, due to their different potential temperature and stratification.

In conclusion, we have shown that it is possible to simulate in a realistic way the local modulations of the katabatic flow in the area of Terra Nova Bay, by taking into account high-resolution topographic features, which include the characteristics of the catchment area and the slope and width of the individual valleys. Even finer resolution is needed, however, to model correctly the effects associated with very narrow valleys. Other more general questions related to the katabatic flow, including its rapid onset and decay, the role of the large-scale circulation and associated wind and pressure fields and the interaction between the large-scale circulation itself and the katabatic winds, are still open problems of Antarctic meteorology that will require further investigation.

6. Acknowledgements

This work was supported by the Programma Nazionale di Ricerche in Antartide. The authors are grateful to G. Mastrantonio and A. Viola (IFA-CNR) for the discussions during the preparation of this work, and to Paolo Grigioni (ENEA) for providing AWS data.

REFERENCES

Argentini, S., Mastrantonio, G., Fiocco, G. and Ocone, R. 1992. Complexity of the wind field as observed by a sodar system and by automatic weather stations on the Nansen Ice Sheet, Antarctica, during summer 1988–89: two case studies. *Tellus* **44B**, 422–429.

Argentini, S., Del Buono, P., Della Vedova, A. M. and Mastrantonio, G. 1995. A statistical analysis of wind in Terra Nova Bay, Antarctica, for the austral summers 1988 and 1989. *Atmos. Res.* **39**, 145–156.

Ball, F. K. 1956. The theory of strong katabatic winds. *Austr. J. Phys.* **9**, 373–386.

Bluestein, H. 1992. *Synoptic-dynamic meteorology in Midlatitudes, Vol. 1. Principles of kinematics and dynamics.* Oxford University Press, Oxford, 444 pp.

Bromwich, D. H. 1989a. An extraordinary katabatic wind regime at Terra Nova Bay, Antarctica. *Mon. Wea. Rev.* **117**, 688–695.

Bromwich, D. H. 1989b. Satellite analyses of Antarctic katabatic wind behavior. *Bull. Am. Meteorol. Soc.* **70**, 738–749.

Bromwich, D. H., Parish, T. R. and Pellegrini, A. 1990a. The katabatic wind regime near Terra Nova Bay, Antarctica. *Antarctic J. US* **25**, 267–269.

Bromwich, D. H., Parish, T. R. and Zorman, C. A. 1990b. The confluence zone of the intense katabatic winds at Terra Nova Bay, Antarctica, as derived from airborne sastrugi surveys and mesoscale numerical modeling. *J. Geophys. Res.* **95**, 5495–5509.

Buzzi, A. and Foschini, L. 2000. Mesoscale meteorological features associated with heavy precipitation in the southern Alpine region. *Meteorol. Atmos. Phys.* **72**, 131–146.

Buzzi, A., Cadelli, R. and Malguzzi, P. 1997. Low-level jet simulation over the Southern Ocean in Antarctica. *Tellus* **49A**, 263–276.

Buzzi, A., Fantini, M., Malguzzi, P. and Nerozzi, P. 1994. Validation of a Limited Area Model in cases of Mediterranean cyclogenesis: surface fields and precipitation scores. *Meteorol. Atmos. Phys.* **53**, 137–153.

Davies, H. C. 1976. A lateral boundary formulation for multilevel prediction models. *Quart. J. Roy. Met. Soc.* **102**, 405–418.

Davolio, S. and Buzzi, A. 2000. Preliminary analysis and simulations of katabatic flow in the vicinity of Terra Nova Bay. *Conference Proc. Italian Research on Antarctic Atmosphere* (eds. M. Colacino, G. Giovannelli and L. Stefanutti). Società Italiana di Fisica, Bologna, **69**, 33–44.

Egger, J. 1985. Slope winds and the axisymmetric circulation over Antarctica. *J. Atmos. Sci.* **42**, 1859–1867.

Gallée, H. 1995. Simulation of mesocyclonic activity in the Ross Sea, Antarctica. *Mon. Wea. Rev.* **123**, 2051–2069.

Gallée, H. 1996. Mesoscale atmospheric circulations over the southwestern Ross Sea sector, Antarctica. *J. Appl. Meteorol.* **35**, 1129–1141.

Gallée, H. 1997. Air–sea interactions over Terra Nova Bay during winter: simulation with a coupled atmosphere-polynya model. *J. Geophys. Res.* **102**, D12, 13,835–13,849.

Gallée, H. and Schayes, G. 1994. Development of a three-dimensional meso-γ primitive equation model: katabatic winds simulation in the area of Terra Nova Bay, Antarctica. *Mon. Wea. Rev.* **122**, 671–685.

Geleyn, J. F. and Hollingsworth, A. 1979. An economical analytical method for the computation of the interaction between scattered and line absorption of radiation. *Contrib. Atmos. Phys.* **52**, 1–16.

Georgelin, M. P., Bougeault, P., Black, T., Brzovic, N., Buzzi, A., Calvo, J., Cassé, V., Desgagné, M., El-Khatib, R., Geleyn, J. F., Holt, T., Hong, S.-Y., Kato, T., Katzfey, J., Kurihara, K., Lacroix, B., Lalaurette, F., Lemaitre, Y., Mailhot, J., Majewsky, D., Malguzzi, P., Masson, V., McGregor, J., Minguzzi, E., Paccagnella, T. and Wilson, C. 2000. The second COMPARE exercise: a model intercomparison using a case of a typical mesoscale orographic flow, the PYREX IOP3. *Quart. J. Roy. Met. Soc.* **126**, 991–1030.

Gyakum, J. R., Carrera, M., Zhang, D.-L., Miller, S., Caveen, J., Benoit, R., Black, T., Buzzi, A., Chouinard, C., Fantini, M., Folloni, C., Katzfei, J. J., Kuo, Y.-H., Lalaurette, F., Low-Nam, S., Mailhot, J., Malguzzi, P., McGregor, J. M., Nakamura, M., Tripoli, G. and Wilson, C. 1996. A regional model intercomparison using a case of explosive oceanic cyclogenesis. *Weather and Forecasting* **11**, 521–543.

Kain, J. S. and Fritsch, J. M. 1990. A one-dimensional entraining/detraining plume model and its application in convective parameterization. *J. Atmos. Sci.* **47**, 2874–2802.

Leheman, R. 1993. On the choice of relaxation coefficients for Davies' lateral boundaries scheme for regional weather prediction models. *Meteorol. Atmos. Phys.* **52**, 1–14.

Malguzzi, P. and Tartaglione, N. 1999. An economical second order advection scheme for explicit numerical weather prediction. *Quart. J. Roy. Met. Soc.* **125**, 2291–2304.

Parish, T. R. 1988. Surface winds over the Antarctic continent: a review. *Rev. Geophys.* **25**, 1, 169–180.

Parish, T. R. 1992. On the role of Antarctic katabatic winds in forcing large-scale tropospheric motions. *J. Atmos. Sci.* **49**, 15, 1374–1385.

Parish, T. R. and Waight, K. T. 1987. The forcing of Antarctic katabatic winds. *Mon. Wea. Rev.* **115**, 2214–2226.

Parish, T. R. and Bromwich, D. H. 1989. Instrumental aircraft observations of the katabatic wind regime near Terra Nova Bay. *Mon. Wea. Rev.* **117**, 1570–1585.

Parish, T. R. and Bromwich, D. H. 1990. Numerical simulation of the katabatic wind circulation over the Antarctic continent. *Antarctic J. US* **25**, 262–264.

Pettré, P. and André, J. C. 1991. Surface-pressure change through Loewe's phenomena and katabatic flow jumps: study of two cases in Adelie Land, East Antarctica. *J. Atmos. Sci.* **48**, 557–571.

Ritter, B. and Geleyn, J. F. 1992. A comprehensive radiation scheme for numerical weather prediction models with potential applications in climate simulations. *Mon. Wea. Rev.* **120**, 303–325.

Viola, A., Rossini, L., Mastrantonio, G., Tagliazucca, M., Argentini, S., Banzi, M., Cardillo, F., Di Donfrancesco, G., Georgiadis, T., Giannini, L., Pellegrini, A. and Trivellone, G. 1996. The boundary layer field experiment in the area of Terra Nova Bay, during the summer 1994–95. *Conference Proc. Italian Research on Antarctic Atmosphere* (eds. M. Colacino, G. Giovannelli and L. Stefanutti). Società Italiana di Fisica, Bologna, **51**, 11–23.

Viola, A. P., Petenko, I., Mastrantonio, G., Argentini, S. and Bezverhnii, V. 1999. Diurnal variations of the temperature and their influence on wind regime in a confluence zone of Antarctica. *Meteorol. Atmos. Phys.* **70**, 133–140.